http://ansinet.com/itj

ITJ

ISSN 1812-5638

INFORMATION TECHNOLOGY JOURNAL

ANSInet
Asian Network for Scientific Information
308 Lasani Town, Sargodha Road, Faisalabad - Pakistan

Information Technology Journal 12 (5): 1011-1017, 2013
ISSN 1812-5638 / DOI: 10.3923/itj.2013.1011.1017

Continuous Optimal Terminal Proximity Guidance Algorithm for Autonomous Rendezvous and Docking

[1,2]Jia Jie, [1]Yao Yu and [1]Ma Kemao
[1]Control and Simulation Center, School of Astronautics, Harbin Institute of Technology, Harbin 150080, China
[2]School of Civil Engineering, Northeast Forestry University, Harbin, 150040, China

Abstract: In the terminal proximity stage of autonomous rendezvous and docking, two kinds of continuous optimal guidance algorithms are developed to overcome the influence of the following terms, the uncertainty of the system model, the noise of the relative information measurements and thrust misalignment on relative guidance accuracy. First of all, a glide slope scheme widely used is introduced to plan the ideal terminal proximity trajectory. By using this assumption the ideal relative position and velocity can be determined beforehand. And then, the tracking error equations for V-bar approach are derived. So, the guidance problem is transformed to synthesize a controller to eliminate the tracking error to zero. Modern control methods are applied to design the H_2/H_∞ controller. The LMI (linear matrix inequalities) technology is adopted here to get the final solution for optimal controllers. Simulation based on the solution obtained though MATLAB LMI toolbox is performed on a scenario of the rendezvous and docking final proximity stage. The simulation results verify the validity and superiority of the H_∞ design method for the terminal proximity of autonomous rendezvous and docking.

Key words: Autonomous rendezvous and docking, terminal proximity, H_2/H_∞ control, linear matrix inequalities, glide slope

INTRODUCTION

Autonomous rendezvous and docking is more and more important nowadays for orbital service, such as fuel injection, solar array replacement and hardware faults repair, etc., Until today almost all successful rendezvous and docking are manned except for orbital express of Boeing Company. The successful demonstration of the two-spacecraft system is part of an ongoing Defense Advanced Research Projects Agency (DARPA) mission to validate on-orbit servicing capabilities (Mokuno *et al*., 2004). The orbital express demonstration program realized the first autonomous proximity process along with R-bar and V-bar. Previous to the critical milestone, The National Space Development Agency of Japan (NASDA) performed unmanned autonomous rendezvous docking (RVD) experiments (Ohkami and Kawano, 2003) using the Engineering Test Satellite VII (ETS-VII) in 1998 and 1999. Also, many researchers had done a lot of work on this problem. Philip and Ananthasayanam (2003) adopted phase-plane control technique to control the relative position; Ortega and Giron-Sierra (1998) used a gene-fuzzy controller performing the closed-loop operations autonomously and a genetic algorithm tool to optimize the controller so as to reduce docking time and fuel consumption; Ma *et al.* (2006) adopted Pontryagin's maximum principle to generate the optimal approaching trajectory and the corresponding set of the control force/torque profiles. Gao *et al.* (2009) designed a H_∞ state-feedback controller via Lyapunov approach to guarantee that the closed-loop system is stability for multi-objective. Zhan *et al*. (2012) investigated the reliable impulsive control problem for autonomous spacecraft rendezvous under the orbital uncertainty and possible thruster faults via Lyapunov theory and genetic algorithms (GA). Qi and Jia (2012) studied constant thrust rendezvous and the optimal rendezvous time by using continuous genetic algorithm. Ma *et al.* (2012) presented a reliable, multi-objective and state-feedback controller design algorithm for trajectory-tracking of circular-orbit rendezvous. Lian *et al.* (2012) researched a fixed-time glide slope guidance algorithm for approaching a target vehicle on a quasi-periodic halo orbit in real Earth-Moon system. Yang *et al.* (2012) proposed a novel approach to spacecraft impulse autonomous rendezvous by using genetic algorithms based on the Clohessy-Wiltshire equations.

Corresponding Author: Jia Jie, Control and Simulation Center, Harbin Institute of Technology, Harbin 150080, China

In these literatures, the relative motion equations are linearized. But the uncertainty of the relative model because of linearizing is ignored. In our study, the study is to solve the terminal proximity guidance problem taking the uncertainty of the relative model into account. Besides the measurement noise of relative velocity and position, the misalignment of the thruster is also taken into account.

PROBLEM FORMULATION

In this section, a glide slope scheme (Hablani *et al*., 2001) is presented to predetermine the terminal proximity relative trajectory of chaser spacecraft. Then, the tracking error equations are derived and the guidance problem is transformed to a controller design problem to eliminate the tracking error.

The terminal proximity trajectory plan: Suppose there is a target spacecraft in a circle orbit referring to Fig. 1. A right-handed local-vertical-local horizontal (LVLH) frame is attached to the target center of mass, with the z-axis downward along the vector to the center of mass of the earth; the x-axis along the target velocity vector v and perpendicular to the z-axis and the y-axis completing the right-handed frame.

In the LVLH frame, the location of chaser spacecraft is (x,y,z) and its velocity is V_x, V_y, V_z. When a chaser spacecraft approaches the target, its relative velocity must be diminished to safe limits. This requirement is fulfilled by designing a guidance trajectory where the range rate is proportional to the range. We adopt a glide slope scheme which is illustrated in Fig. 2. As the distance-to-go $\rho(t)$ is diminished, the speed $\dot{\rho}$ must diminish with it. $\dot{\rho}$ is obtained by differentiating ρ. Since, the proximity time is very short, we can treat the LVLH frame as an inertial non-rotating frame. Suppose the following linear relationship between ρ and $\dot{\rho}$ is satisfied.

$$\dot{\rho} = \alpha\rho + \dot{\rho}_T \tag{1}$$

where, α is the slope of $\dot{\rho}$ vs. ρ, when the chaser spacecraft approaches the target spacecraft in the terminal stage of rendezvous and docking, two ways are usually be used, which are R-bar and V-bar. In our study, the V-bar approach is used mainly. The algorithm used here is also valid for R-bar. According to Eq. 1, the following equation can be given:

$$V_x(t) = ax + \dot{x}_T \tag{2}$$

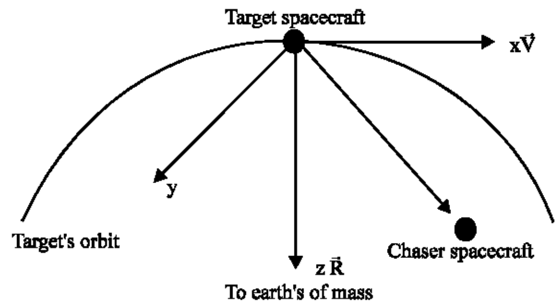

Fig. 1: Chaser's relative motion referring to target in LVLH

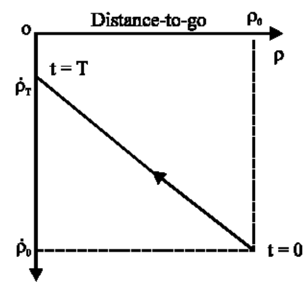

Fig. 2: Reduction of the velocity $\dot{\rho}$ with time

where:

$$a = (\dot{\rho}_0 - \dot{\rho}_T)/\rho < 0$$

In the V-bar approach way, the chaser's velocity component V_y and V_z must be limited to zero. The boundary conditions of x and V_x are:

$$\begin{aligned} t = 0 &: x = x_0, V_x = V_{x0} < 0 \\ t = T &: x = 0, V_x = V_{xT} < 0 \end{aligned} \tag{3}$$

With the boundary conditions Eq. 3, the solution to Eq. 2 is:

$$x(t) = x_0 e^{at} + V_{xT}(e^{at} - 1)/a \tag{4}$$

And the proximity time T = $(1/\alpha)$ in (V_{xT}/V_{x0}). When the chaser's velocity component V_x conform to Eq. 4 and V_y, V_z are limited to zero, the chaser will approach the target along with V-bar. The command velocity, Eq. 2, corresponds to a varying commanded acceleration $\dot{V}_x = aV_x$ and since V_x is decreasing with time, the acceleration decreases with time. These features are desirable for proximity process.

Tracking error equation: In the LVLH coordinate system, the relative motion of the chaser spacecraft located at a station (x,y,z), where y and z are much smaller than the target orbit radius, is governed by the following C-W equations:

$$\begin{aligned} \ddot{x} &= 2\omega\dot{z} + u_x \\ \ddot{y} &= -\omega^2 y + u_y \\ \ddot{z} &= -2\omega\dot{x} + 3\omega^2 z + u_z \end{aligned} \tag{5}$$

where, u_x, u_y and u_z are the acceleration components generated by the chaser's actuator in the xyz frame attached to the target.

Because the cross-track motion is uncoupling, the relative motion is considered in the x-z plane. By differentiating Eq. 4, the velocity command $\dot{x}_{command}$ and the acceleration command $\ddot{x}_{command}$ can be obtained.

$$\begin{aligned} \dot{x}_{command} &= ax_{command} + V_{xT}, \\ \ddot{x}_{command} &= (a^2 x_0 + aV_{xT})e^{at} \\ &= a^2 x_{command} + aV_{xT} = a\dot{x}_{command} \end{aligned} \tag{6}$$

In the V-bar approach process, $\dot{z}_{command}$ and $\ddot{z}_{command}$ are both zero.The position and velocity tracking errors are defined as the state space variables:

$$\begin{aligned} x_1 &= x_{command} - x, x_2 = z_{command} - z \\ x_3 &= \dot{x}_{command} - \dot{x}, x_4 = \dot{z}_{command} - \dot{z} \end{aligned} \tag{7}$$

Thus, the tracking error equations can be achieved, which can be transformed standard state space equations:

$$\begin{aligned} \dot{X} &= AX + B_2 U + B_1 w \\ Z &= CX + DU \end{aligned} \tag{8}$$

$$A = \begin{bmatrix} 0 & 0 & 1 & 0 \\ 0 & 0 & 0 & 1 \\ 0 & 0 & 0 & 2\omega \\ 0 & 3\omega^2 & -2\omega & 0 \end{bmatrix}, B_1 = \begin{bmatrix} 0 & 0 & 0 & 0 & 0 \\ 0 & 0 & 0 & 0 & 0 \\ 1 & 0 & 0 & 0 & 2\omega \\ 0 & 1 & 3\omega^2 & -2\omega & 0 \end{bmatrix}$$
$$B_2 = \begin{bmatrix} 0 & 0 \\ 0 & 0 \\ 1 & 0 \\ 0 & 1 \end{bmatrix}, C = \begin{bmatrix} qI_{4\times4} \\ 0_{2\times4} \end{bmatrix}, D = \begin{bmatrix} 0_{4\times2} \\ rI_{2\times2} \end{bmatrix} \tag{9}$$

where:

$$\begin{aligned} X &= [x_1\ x_2\ x_3\ x_4]^T, Z = [qI_{4\times4}\ rI_{2\times2}U]^T \\ U &= [a\dot{x}_{command} - u_x\ \ 2\omega\dot{x}_{command} - u_z]^T \\ w &= [w_x\ w_z\ \delta x_2\ \delta x_3\ \delta x_4]^T \end{aligned} \tag{10}$$

where, w_x and w_z represent the model error because of linearizing Eq.5 and actuating error is caused by thruster misalignment. δ_{x2}, δ_{x3} and δ_{x4} represent measurement noise of x_2, x_3 and x_4. q,r represent the weighting scale of the tracking error and control input, respectively in the measurement output equation.

Now the tracking problem is transformed to a controller design problem. If the related study can find a controller which can drive the tracking error to zero and constrain the effect of w, then the chaser will glideslope to the target along with V-bar in a very safe mode.

H_2 AND H_∞ CONTROLLERS DESIGN

The problem of the V-bar proximity is transformed to a problem that the tracking error is eliminated in section 2. With the application of modern control theory, the controllers can be designed to eliminate the tracking error, also to constrain the effect of the perturbation of relative motion model, the relative measurement noise and the misalignment of thrusters on the terminal proximity guidance accuracy.

H_2 controller design: Through designing state feedback control law for Eq. 8, the closed-loop system Eq. 11 is stable and the transfer function matrix satisfies in Eq. 12 for an arbitrarily given positive scalar γ_1.

$$U = KX \tag{11}$$

$$\begin{cases} \dot{x} = (A + B_2 K)U + B_1 w \\ z = (C + DK)X \end{cases} \tag{12}$$

$$\| G_{wz} \|_2 = \| (C + DK)[sI - (A + B_2 K)^{-1}]B_1 \|_2 < \gamma_1 \tag{13}$$

This is a normal H_2 state feedback control problem which can be solved with the Linear Matrix Inequality (LMI) technology easily.

H_∞ controller design: In the subsection above, it is unnecessary to the tracking error is eliminated in all frequency. The scheme of allowing the high frequency error to a bit larger at a reasonable level and the low frequency error to near zero will save a lot of control energy. So, the tracking problem can be handled through introducing a tracking model and using H_∞ control theory. The following figure illustrates the H_∞ tracking method.

Here the relative dynamics state space model is derived form the classical C-W equations. To design the H_2 tracking controller, the relative motion is only considered in x-z plane. Choosing $[x,z,V_z,V_z]^T$ as state space variables, $[u_x, u_z]^T$ as input, the measurement output is state space variables. $d_{Model\,Uncertainty}$, $d_{measurement}$ and d_u

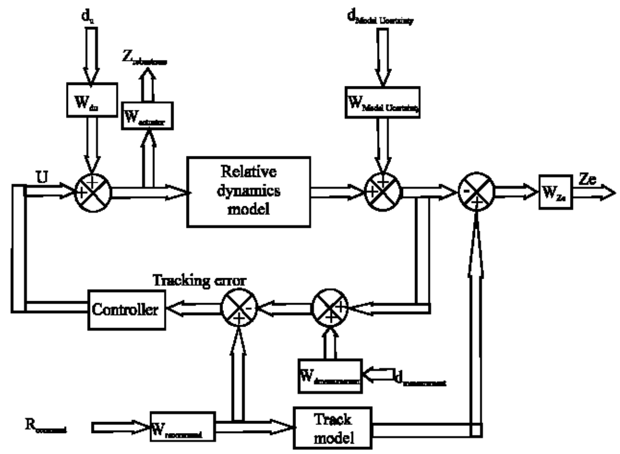

Fig. 3: Flow chart of H_∞ tracking controller design

represent, respectively the uncertainty of the relative model, the relative measurement noise and the actuator disturbance generated by the misalignment of thrusters. $W_{dModelUcertainty}$, W_{du}, $W_{dmeasurement}$, $W_{Rcommand}$, $W_{actuator}$ and W_{ze} are weighting functions. $R_{command}$ is the predetermined relative position and velocity in section 2. $Z_{robustness}$ and Z_e are the evaluation performance output and the former one represents the robust stability of relative dynamics model in present of additive uncertainty and the later one represents model reference tracking error. Actually the terminal proximity problem is transformed to a model matching problem. The objective of the closed-loop system is to match the defined model in Fig. 3. For excellent command tracking response, the closed-loop system should respond like a well-damped second-order system. G_{ZW}, which is the form of transfer function matrix, is defined from exogenous influences (reference command, model uncertainty, measurement noise, thruster misalignment) to the regulated variables (model reference tracking error and control input signal).

The equation is obtained below:

$$[Z_{robustness}, z_e]^T = G_{zw}[R_{command}, d_{ModelUcertainty}, d_{measurement}, d_u]^T \quad (14)$$

So, the study is to find the controllers K which stabilizes the closed-loop system and conforms to the H_∞ norm const rain:

$$\| G_{zw} \|_\infty < \gamma_2 \quad (15)$$

GET CONTROLLER SOLUTION VIA LMI

Equation 12 and 14 are H_2 and H_∞ norm constrain exogenous influences to regulated variables, respectively. γ_1, γ_2 are the upper norm bounds. γ_1, γ_2 can be optimized on controller sets which stabilize the closed-loop system to get the optimal controller. These problems are lack of an analytical solution, fortunately the linear matrix inequality method can solve the H_2 and H_∞ problem in a union computing frame (Gahinet *et al*., 1995). H_2 and H_∞ norm constrain are transformed to LMI constrain on controllers. Solving the LMI constrains problem is a convex optimization problem. Efficient interior-point algorithms are now available to solve the generic LMI problems with a polynomial-time worst-case complexity. So, reducing the tracking error eliminating problem to LMI problems can be considered as a practical solution to this problem.

NUMERICAL SIMULATION RESULTS

As a numerical example, the slope of $\dot{\rho}$ vs. ρ α = -0.004 is chosen. The initial condition of the chaser location and velocity are (50 m, 0.0), respectively. So, Eq. 16 can be obtained:

$$\begin{aligned} &x_{command} = 58.75e^{-0.004t} - 8.75, z_{command} = 0 \\ &V_{xcommand} = -0.235t, V_{zcommand} = 0 \end{aligned} \quad (16)$$

The chaser spacecraft mass is 1000 kg and the thrust force is 10 N. The target's orbital height is 500 km and its eccentricity is zero. The relative measurement noise is 0.03 m (3σ) and the velocity measurement noise is 0.01 m sec^{-1}. Since, the thrusters work discretely, the continuous control input have to be transformed to discrete form. The PWPF technology is adopted to perform this transformation. Following is the numerical simulation results.

Simulation with H_2 controller: The weighting scale q = 10, r = 1 are chosen, the state feedback controller is obtained through the MATLAB function matrix form LMI toolbox. The numerical simulation results are Fig. 4 and 5.

Simulation with H_2 controller: The weighting functions and reference model are obtained as follow:

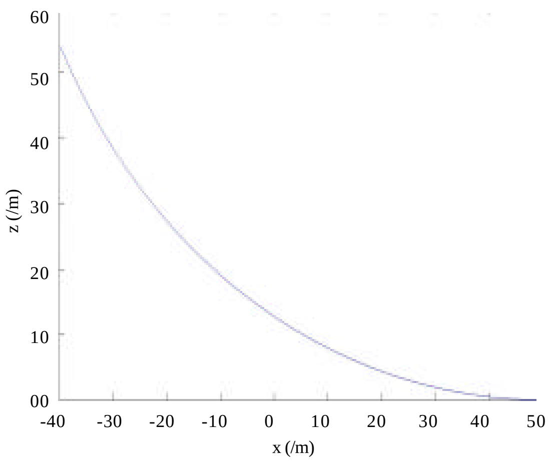

Fig. 4: Projection of uncontrolled relative motion in x-z plane

$$
\begin{aligned}
& W_{dModel\,Ucertainty} = \frac{0.25s+0.05}{0.5s+1} I_{4\times4},\ W_{actuator} = 1\times10^{-3} I_{2\times2} \\
& W_{ze} = \mathrm{diag}([100\,100\,50\,50]) \times \frac{1}{s+1} \\
& W_{dmeasurement} = 333 \frac{s+1}{s+10} I_{2\times2} \\
& G_{trackmodel} = \frac{2.25}{s^2+2.121s+2.25}
\end{aligned}
\qquad (17)
$$

All LMI-related here computation are performed with the function h-infinity from the LMI Control Toolbox. K (s) is a matrix which has two rows and four columns. The numerical simulation results are in Fig. 6.

RESULTS

The problem on autonomous rendezvous and docking is studied in previous literature including controlling the relative position, reducing docking time and fuel consumption and optimal approaching trajectory etc. Among these researches, the model is established without considering the uncertainty of the relative model, the measurement noise of relative velocity and position and the misalignment of the thruster. Based on the factors, the continuous optimal guidance algorithms are

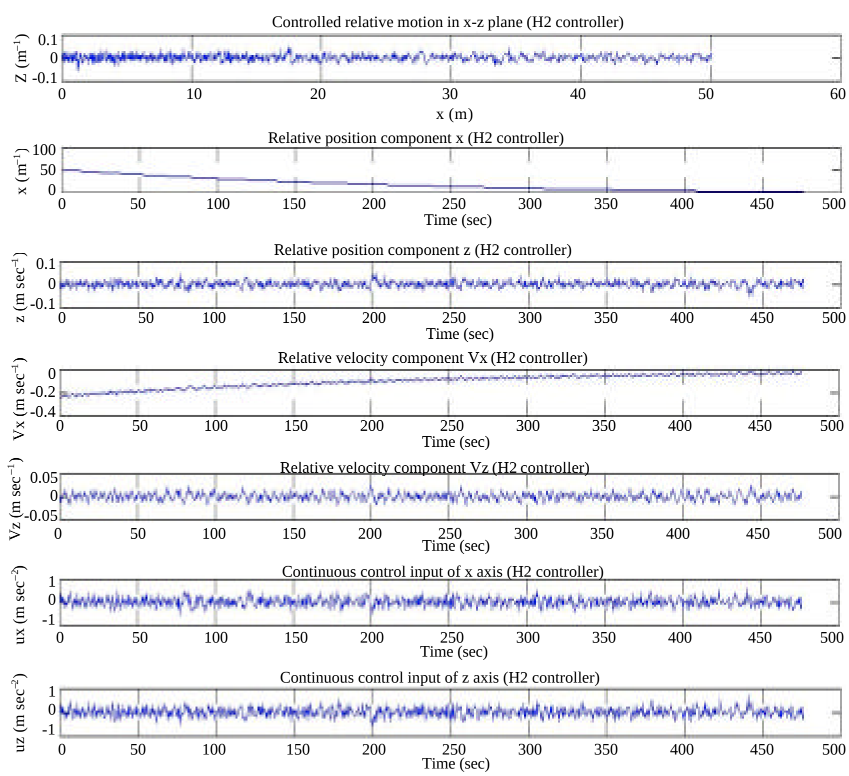

Fig. 5: Relative position, relative velocity component and control input for in x axis and y axis with H_2 controller

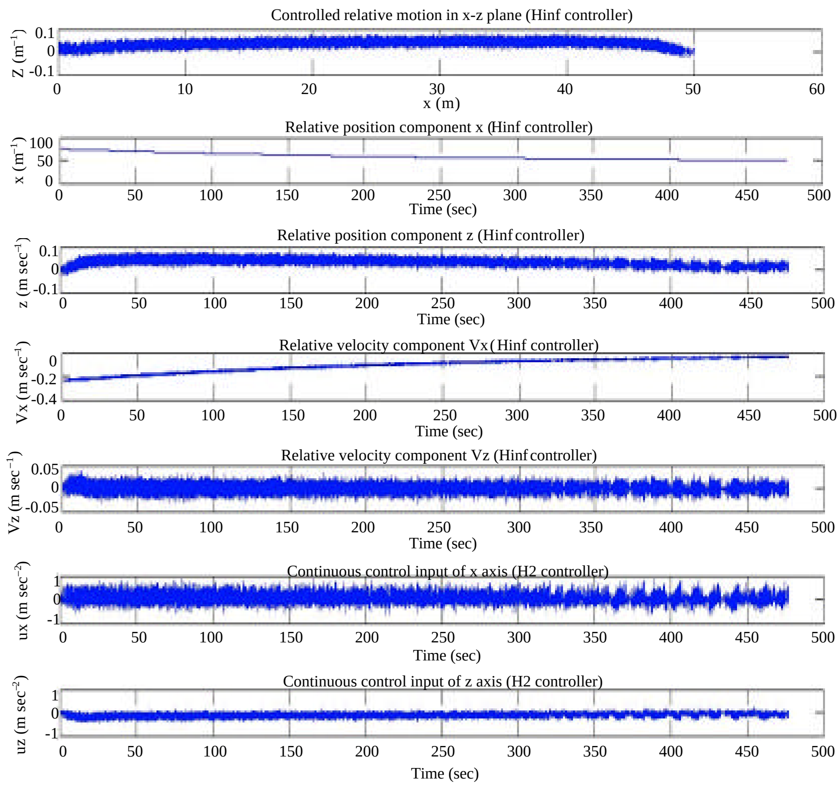

Fig. 6: Relative position, relative velocity component and control input for in x axis and y axis with H_2 controller

studied via the design of H_2/H_∞ controllers. From the simulation results in Fig. 4-6, the tracking error can be eliminated near to zero by two kinds of H_2 and H_∞ controllers. The former keeps the tracking error under 0.05 m. Actually the H_2 controller is a PD controller as a form of PID control method. But the tracking error is larger at initial stage for later controller, under 0.08 m, as the chaser get closer to the target, the tracking error become smaller and smaller. At the last stage tracking error is under 0.05 m. These phenomena state that adopting the reference tracking model can allow the high frequency error is a bit larger and low frequency error is smaller. The advantage of the scheme is that it saves a mount of fuel. The last two sub-figures of Fig. 5, 6 can testify this point of view. Another feature of the H_∞ controller is that the exogenous influences are constrained to a concentrate area. So, the curves are dense. By choosing proper weighting function, the desirable tracking performance can be obtained by using H_∞ design method at lower fuel expense. But it needs the information of the system in frequency domain.

CONCLUSION

Two kinds of continuous optimal guidance algorithms for spacecraft rendezvous and docking subject to the model uncertainty, the noise of the relative information measurements and thrust misalignment is present in this study. By using modern control methods, the guidance problem has been transformed into the H_2/H_∞ controller design with LMI technology. The final solution for optimal controllers is obtained. The simulation results indicates that the methods of the proposed controller design are validity and superiority.

ACKNOWLEDGMENT

This study is partially supported the National Natural Science Foundation of China (under the Project Number 61074160 and 61174001).

REFERENCES

Gahinet, P., A.J. Laub and M. Chilali, 1995. The LMI Control Toolbox. The Math- Works Inc., USA.

Gao, H., X. Yang and P. Shi, 2009. Multi-objective robust H-infinity control of spacecraft rendezvous. IEEE Trans. Control Syst. Technol., 17: 794-802.

Hablani, H.B., M. Tapper and D.B. David, 2001. Guidance algorithms for autonomous rendezvous of spacecraft with a target vehicle in circular orbit. Proceedings of the AIAA Guidance, Navigation and Control Conference and Exhibit, August 2001, Montreal, Canada, pp: 1-15.

Lian, Y., Y. Meng, G. Tang and L. Liu, 2012. Constant-thrust glideslope guidance algorithm for time-fixed rendezvous in real halo orbit. Acta Astronautica, 79: 241-252.

Ma, L., X. Meng, Z. Liu and L. Du, 2012. Multi-objective and reliable control for trajectory-tracking of rendezvous via parameter-dependent Lyapunov functions. Acta Astronautica, 81: 122-136.

Ma, Z., O. Ma and B.N. Shashikanth, 2006. Optimal control for spacecraft to rendezvous with a tumbling satellite in a close range. Proceedings of the 2006 IEEE/RSJ International Conference on Intelligent Robots and Systems, October 9-15, 2006, Beijing, pp: 4109-4114.

Mokuno, M., I. Kawano and T. Suzuki, 2004. In-orbit demonstration of rendezvous laser radar for unmanned autonomous rendezvous docking. IEEE Trans. Aerosp. Electron. Syst., 40: 617-626.

Ohkami, Y. and I. Kawano, 2003. Autonomous rendezvous and docking by engineering test satellite VII: A challenge of Japan in guidance, navigation and control-Breakwell memorial lecture. Act Astrona, 53: 1-8.

Ortega, G. and J.M. Giron-Sierra, 1998. Geno-fuzzy control in autonomous servicing of a space station. Eng. Appl. Artificial Intell., 11: 383-400.

Philip, N.K. and M.R. Ananthasayanam, 2003. Relative position and attitude estimation and control schemes for the final phase of an autonomous docking mission of spacecraft. Act Astrona, 52: 511-522.

Qi, Y.Q. and Y.M. Jia, 2012. Constant thrust fuel-optimal control for spacecraft rendezvous. Adv. Space Res., 49: 1140-1150.

Yang, X.B., J.Y. Yu. and H.J. Gao, 2012. An impulse control approach to spacecraft autonomous rendezvous based on genetic algorithms. Neurocomputing, 77: 189-196.

Zhan, L., X. Yang and H. Gao, 2012. Autonomous impulsive rendezvous for spacecraft under orbital uncertainty and thruster faults. J. Franklin Inst., 10.1016/j.jfranklin.2012.07.002